



**HAL**  
open science

## Study of Defects in GaAs by 2D-ACAR Positron Annihilation

A.A. Manuel, R. Ambigapathy, P. Hautojärvi, K. Saarinen, C. Corbel

► **To cite this version:**

A.A. Manuel, R. Ambigapathy, P. Hautojärvi, K. Saarinen, C. Corbel. Study of Defects in GaAs by 2D-ACAR Positron Annihilation. Journal de Physique IV Proceedings, 1995, 05 (C1), pp.C1-73-C1-80. 10.1051/jp4:1995108 . jpa-00253544

**HAL Id: jpa-00253544**

**<https://hal.science/jpa-00253544>**

Submitted on 4 Feb 2008

**HAL** is a multi-disciplinary open access archive for the deposit and dissemination of scientific research documents, whether they are published or not. The documents may come from teaching and research institutions in France or abroad, or from public or private research centers.

L'archive ouverte pluridisciplinaire **HAL**, est destinée au dépôt et à la diffusion de documents scientifiques de niveau recherche, publiés ou non, émanant des établissements d'enseignement et de recherche français ou étrangers, des laboratoires publics ou privés.

## Study of Defects in GaAs by 2D-ACAR Positron Annihilation

A.A. Manuel, R. Ambigapathy, P. Hautojärvi\*, K. Saarinen\* and C. Corbel\*\*

*Université de Genève, Département de Physique de la Matière Condensée, 24, quai E. Ansermet, CH-1211 Genève 4, Switzerland*

*\* Laboratory of Physics, Helsinki University of Technology, SF 02150 Espoo, Finland*

*\*\* Centre d'Etudes Nucléaires, INSTN, F 91191 Gif-sur-Yvette Cedex, France*

**Abstract:** We describe the two dimensional angular correlation of positron annihilation radiation (2D-ACAR) method and show that it can be advantageously used to study the electronic structure of defects, in addition to standard positron lifetime and Doppler broadening measurements. Using annihilation fractions determined by lifetime measurements, we separate 2D-ACAR distributions for negatively charged and neutral arsenic vacancies in n-type GaAs. In electron-irradiated semi-insulating GaAs, we present 2D-ACAR results for the negatively charged gallium vacancy and for positron Rydberg states induced by gallium antisites. The 2D-ACAR for delocalized positrons, needed in the separation process, has been obtained from measurements on as-grown semi-insulating GaAs. Our results outline the capabilities of the 2D-ACAR technique when it is applied to the study of defects: the electronic structure in the vacancies are found to be well described by recent molecular dynamics calculations. The method also provides information about atomic relaxations around the vacancy sites, they are in agreement with the calculated relaxations. We conclude that the 2D-ACAR method is a promising tool to investigate defects in semiconductors.

### 1. INTRODUCTION

Defects play an important role in the electronic properties of semiconductors [1]. Even in very small concentrations they produce significant effects as they interact with the free carriers, acting as scattering centers, traps or recombination centers. It is thus important to investigate the defects. Their characterization, as well as the understanding of their electronic properties, is an active field of research, with a large technological impact as the scale of the devices is constantly reducing. Different classes of defects are to be found in semiconductors: impurities, vacancies, interstitials, antisites (in compound semiconductors) and their complexes. Their existence depends on the mode of growth, thermal treatment, ion implantation, irradiation, surface and interface treatments.

Due to the large variety of effects they produce, defects are studied and characterized with various techniques, each providing a specific piece of information. The classical techniques sensitive to the electronic properties are the electrical and optical measurements and electron paramagnetic resonance. Positron annihilation has recently proved to be a useful tool to perform numerous detailed investigations of defects in semiconductors [2][3][4]. Positrons are sensitive to the charge distribution in solids. In the case of an attractive site, like a neutral or negatively charged vacancy, trapping of positrons may occur and the annihilation characteristics will therefore be directly related to this local environment.

The positron annihilation technique provides three measurable quantities: positron lifetime, Doppler broadening of the annihilation radiation and angular correlation of the annihilation radiation (ACAR). The positron lifetime is proportional to the electron density at the annihilation site while Doppler and ACAR techniques provide information on the electronic structure through the momentum distribution of the annihilating electron - positron pairs. The latter two techniques also possess a directional resolving power when single crystals are investigated. This property is rather unique among the probes mentioned above and is specially attractive with the high resolution two dimensional angular correlation of annihilation radiation (2D-ACAR) geometry discussed in this paper.

The plan of the paper is the following. In Section 2 we describe the 2D-ACAR technique. We intentionally omit descriptions of lifetime and Doppler techniques as they are to be found elsewhere in these proceedings [5].

In Section 3 we discuss positron states for various defects in GaAs. We focus on different charge states of native As vacancy ( $V_{As}$ ) and the negatively charged Ga vacancy ( $V_{Ga}$ ). We also discuss positron Rydberg states induced by Ga antisites ( $Ga_{As}$ ). We briefly present how lifetime measurements provide accurate values of the annihilation fractions in the different defects. More details are given elsewhere in these proceedings [5].

In Section 4 we present 2D-ACAR measurements performed in semi-insulating (SI), Si-doped and electron-irradiated GaAs. Using the partial annihilation fractions determined in Section 3, it is possible to extract the 2D-ACAR components of the various defects. We have determined 2D-ACAR distributions for  $V_{As}$ ,  $V_{As}^0$ ,  $V_{Ga}^{3-}$  and Rydberg states around  $Ga_{As}^{2-}$ .

Before concluding in Section 6, we discuss the results in Section 5, where it is shown that the shape of the 2D-ACAR distribution reflects the local electronic structure at the annihilation site. When positrons annihilate freely in the bulk, the 2D-ACAR probes the covalent bonds and other electronic states, providing precise information on the electron momentum distribution in the defect-free crystal. When positrons annihilate in a defect, we observe a quite different 2D-ACAR distribution. This demonstrates that the technique is sensitive and well suited to the study of the defects in semiconductors. From our measurements, we deduce the following points:

1. The electronic structure of monovacancies is more isotropic than that of the bulk. To interpret this result, Molecular Dynamics calculations are required. A recent calculation [6], using the Car-Parinello approach [7], has shown that a substantial agreement exists between experiments and theory.
2. We have obtained direct experimental evidence for a large inward relaxation of  $V_{As}$ .
3. Positron Rydberg states induced by  $Ga_{As}^{2-}$  antisites prove to be quite delocalized. Their electronic structure is very similar to the defect free GaAs.

A more detailed description of most of this work may be found elsewhere [8].

## 2. THE 2D-ACAR TECHNIQUE

The 2D-ACAR technique [9] measures  $N(p_x, p_y)$  the projection along the  $p_z$  direction of the so-called two-photon momentum density  $\rho^{2\gamma}(\vec{p})$ :

$$N(p_x, p_y) = \int \rho^{2\gamma}(\vec{p}) dp_z \quad (1)$$

In the independent particle approximation  $\rho^{2\gamma}(\vec{p})$ , is given by:

$$\rho^{2\gamma}(\vec{p}) = const \cdot \sum_{n, \vec{k}}^{occ} \left| \int e^{i\vec{p}\cdot\vec{r}} \Psi_{n, \vec{k}}(\vec{r}) \Psi^+(\vec{r}) d^3r \right|^2 \quad (2)$$

where  $\Psi_{n, \vec{k}}$ , and  $\Psi^+$  are the electron and positron wavefunctions ( $n$  and  $\vec{k}$  label the bands and the points in the fundamental cell of the reciprocal lattice, see [10] for a more detailed discussion). The vectors  $\vec{p}$  and  $\vec{k}$  are related by  $\vec{p} = \vec{k} + \vec{G}$ , where  $\vec{G}$  is a reciprocal lattice vector.

As Eq. (2) shows,  $\rho^{2\gamma}(\vec{p})$  is related to the Fourier transform of the overlap of the positron and electron wavefunctions. This means that  $N(p_x, p_y)$  reflects the electronic structure as seen by the positron. If the positron wavefunction is fairly delocalized in the interstitial region, as is the case in a defect-free lattice, we obtain a signal from the valence bands. The inner electronic shells provide a smaller signal because the positron, due to its positive charge, is repelled from the region of the core. If the positron is trapped in a

vacancy, its wavefunction is localized and  $\rho^{2\gamma}(\vec{p})$  provides an insight to the electronic states in the defect. We use this property to investigate the defects states by 2D-ACAR.

As the 2D-ACAR is by nature different from positron lifetime measurements, these two techniques are complementary. Comparing Doppler and 2D-ACAR, which both probe the same physical quantity  $\rho^{2\gamma}(\vec{p})$ , we point out two advantages of 2D-ACAR measurements:

1. It is more informative because it is a 2D distribution, where  $\rho^{2\gamma}(\vec{p})$  is integrated only once, while Doppler measurements  $D(p_x)$  provide a less direct information due to a double integration:

$$D(p_x) = \iint \rho^{2\gamma}(\vec{p}) dp_y dp_z \quad (3)$$

2. The experimental resolution of the 2D-ACAR is much better (of the order of  $0.5 \times 10^{-3} mc$ , where  $m$  is the mass of the electron at rest and  $c$  the speed of the light in vacuum) than for Doppler measurements ( $\sim 4 \times 10^{-3} mc$ ).

The disadvantage of the 2D-ACAR technique is that it requires a longer counting time. Therefore, it is only to be used in conjunction with lifetime and Doppler measurements, which remain important explorative techniques using positrons as probes.

### 3. POSITRON STATES IN GaAs

#### 3.1. n-type GaAs

In n-type GaAs, positron lifetime experiments have shown [11] [12] that the native vacancies undergo two Fermi level controlled transitions. The first transition takes place when the Fermi level goes below 30 meV from the minimum of the conduction band ( $E_c$ ). It is experimentally detected as an increase in the positron lifetime at the vacancy from 257 ps to 295 ps. When the temperature increases, the Fermi level decreases even more and falls below  $E_c - 140$  meV. There occurs a second transition which inhibits the positron from trapping at vacancies. These observations are attributed to transitions in the charge state of the As vacancy:  $V_{As}^- \rightarrow V_{As}^0$  and  $V_{As}^0 \rightarrow V_{As}^+$ .

In a sample of Si-doped n-type GaAs with a carrier concentration of  $6.2 \times 10^{16} \text{ cm}^{-3}$  at 300 K, it is possible, using information obtained from lifetime experiments, to perform a decomposition of the 2D-ACAR measured at the two temperatures of 90 K and 300 K [8].

At 90 K, the 2D-ACAR spectrum  $f^{90}(\vec{p})$  can be decomposed as

$$f^{90}(\vec{p}) = \eta_b f_b^{90}(\vec{p}) + \eta_{V_{As}^-} f_{V_{As}^-}^{90}(\vec{p}) \quad (4)$$

where  $f_b^{90}(\vec{p})$  and  $f_{V_{As}^-}^{90}(\vec{p})$  are the 2D-ACAR fractions of the bulk and of the negative As vacancy, respectively. Here,  $\vec{p}$  denotes the pair of momentum components  $(p_x, p_y)$ , while  $\eta_b$  and  $\eta_{V_{As}^-}$  are the fractions of positrons annihilating in the bulk and at the vacancy with  $\eta_b + \eta_{V_{As}^-} = 1$ . Using lifetime measurements, the value of the trapping fractions have been determined to be  $\eta_b = 0.52$  and  $\eta_{V_{As}^-} = 0.48$ .

At 300 K, the 2D-ACAR distribution  $f^{300}(\vec{p})$  can be decomposed following similar procedures. However, the positron lifetime experiments show that the charge state transition of the As vacancy  $V_{As}^- \rightarrow V_{As}^0$  is not complete [8]. Consequently,  $f^{300}(\vec{p})$  is given by:

$$f^{300}(\vec{p}) = \eta_b f_b^{300}(\vec{p}) + \eta_{V_{As}^0} f_{V_{As}^0}^{300}(\vec{p}) + \eta_{V_{As}^-} f_{V_{As}^-}^{300}(\vec{p}) \quad (5)$$

The annihilation fractions in this case have been determined to be  $\eta_b = 0.50$ ,  $\eta_{V_{As}^0} = 0.35$  and

$$\eta_{V_{As}^-} = 0.15.$$

Once the annihilation fractions are known, the 2D-ACAR distribution of the neutral As vacancy  $f_{V_{As}^0}^{300}(\vec{p})$  can be extracted using Eq. (5). In this decomposition, we use the measurement of the undoped semi-insulating GaAs reference sample at 300 K to determine the bulk distribution  $f_b^{300}(\vec{p})$ . The 2D-ACAR spectrum  $f_{V_{As}^-}^{300}(\vec{p})$  for the negative As vacancy is obtained from the decomposition at 90 K (Eq. (4)) by substituting  $f_{V_{As}^-}^{300}(\vec{p}) = f_{V_{As}^0}^{90}(\vec{p})$ . This substitution is justified as we noticed that the 2D-ACAR distribution of the bulk changed little from 300 K to 90 K. (The small change can be attributed to the thermal expansion of the lattice.) We can thus presume that the distribution of the defect ( $V_{As}^-$ ) similarly does not change substantially from 300 K to 90 K. In this way the 2D-ACAR distributions of both negative and neutral vacancies can be obtained from the original data using the results of lifetime experiments and the decomposition procedures discussed above. The positron trapping by positively charged vacancies like  $V_{As}^+$  has been considered in [13]. It has been found that the trapping coefficient depends on the amplitude of the repulsive Coulomb barrier. For reasonable barriers heights no significant trapping occurs; this is in agreement with the interpretation of the lifetime measurements [11]. This explains why there is no annihilation fraction for  $V_{As}^+$  in Eq. (5).

### 3. 2. Electron-irradiated semi-insulating GaAs

A similar procedure has been used to decompose the 2D-ACAR from a sample of semi-insulating GaAs irradiated with a fluence of  $5 \times 10^{17} \text{ cm}^{-2}$  of 1.5 MeV electrons. Lifetime measurements [14] provide the following decomposition at 90 K:

$$f^{90}(\vec{p}) = \eta_b f_b^{90}(\vec{p}) + \eta_{V_{Ga}^{3-}} f_{V_{Ga}^{3-}}^{90}(\vec{p}) + \eta_{Ga_{As}^{2-}} f_{Ga_{As}^{2-}}^{90}(\vec{p}) \quad (6)$$

where the annihilation fractions have been determined to be  $\eta_b = 0.06$ ,  $\eta_{V_{Ga}^{3-}} = 0.1$  and  $\eta_{Ga_{As}^{2-}} = 0.84$

At 300 K the positron only annihilates from the bulk or at gallium vacancies and the decomposition is given as

$$f^{300}(\vec{p}) = \eta_b f_b^{300}(\vec{p}) + \eta_{V_{Ga}^{3-}} f_{V_{Ga}^{3-}}^{300}(\vec{p}) \quad (7)$$

The trapping fractions at 300 K are  $\eta_b = 0.67$  and  $\eta_{V_{Ga}^{3-}} = 0.33$

As the decompositions given in Eq. (6) and Eq. (7) show, electron irradiation of SI samples results in the production of Ga vacancies and  $Ga_{As}^{2-}$  antisites. The latter defect, which we call shallow trap, acts as a center for the formation of weakly bound positron Rydberg states.

## 4. 2D-ACAR RESULTS

For the 2D-ACAR measurements, we have used a spectrometer composed of high density proportional chambers [15]. The experimental details are given in [8]. The measurements were performed at 90 K and 300 K in the (110) plane of single crystalline samples of 1) semi-insulating, 2) n-type and 3) electron-irradiated GaAs. Using the decomposition procedures described in section 3 we have extracted the 2D-ACAR shown in Figure 1 for bulk GaAs,  $V_{As}^-$ ,  $V_{As}^0$ ,  $V_{Ga}^{3-}$  and Rydberg states around  $Ga_{As}^{2-}$  antisites. The general observation is that the results can be separated into two distinct groups: the first includes bulk GaAs and Rydberg states and the second the three vacancy distributions. The origin of these two groups is explained in section 5.

It is useful to consider the anisotropies of the 2D-ACAR distributions which are obtained by subtracting their cylindrical mean. In Figure 2, we show the anisotropies for bulk GaAs,  $V_{As}^-$ ,  $V_{Ga}^{3-}$  and Rydberg states around  $Ga_{As}^{2-}$  antisites. One notices that in fact the two groups introduced above are characterized by the same topology of anisotropies. What distinguishes them is the intensities of the anisotropies, which are

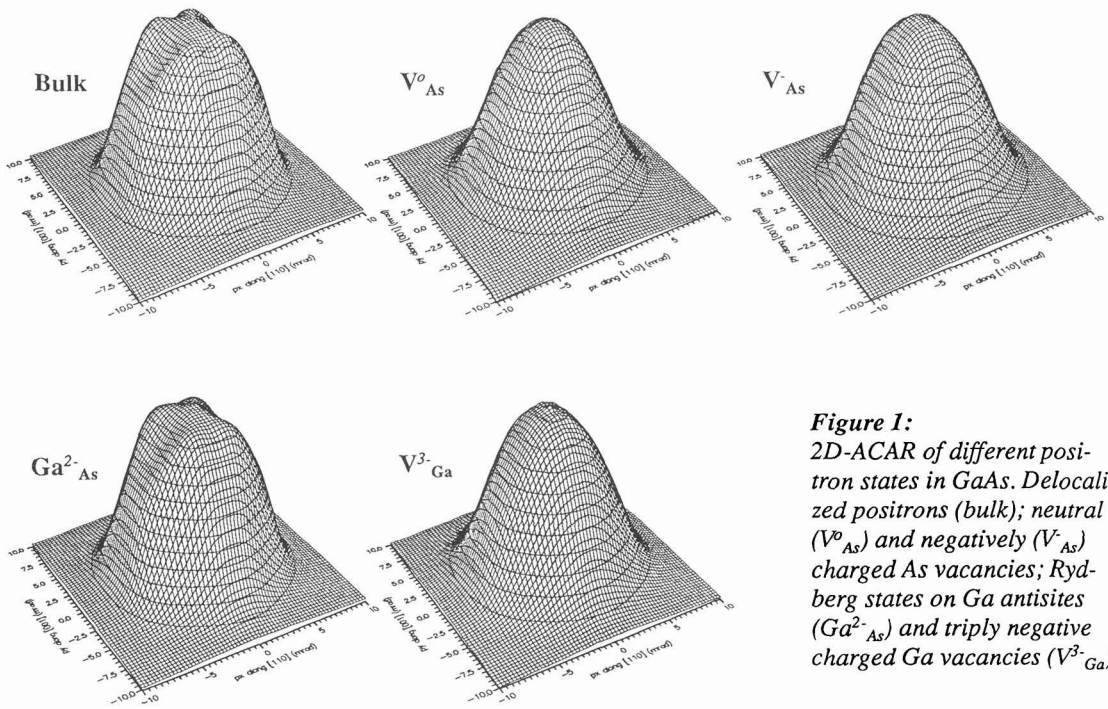


**Figure 1:**  
2D-ACAR of different positron states in GaAs. Delocalized positrons (bulk); neutral ( $V_{As}^0$ ) and negatively ( $V_{As}^-$ ) charged As vacancies; Rydberg states on Ga antisites ( $Ga_{As}^{2-}$ ) and triply negative charged Ga vacancies ( $V_{Ga}^{3-}$ )

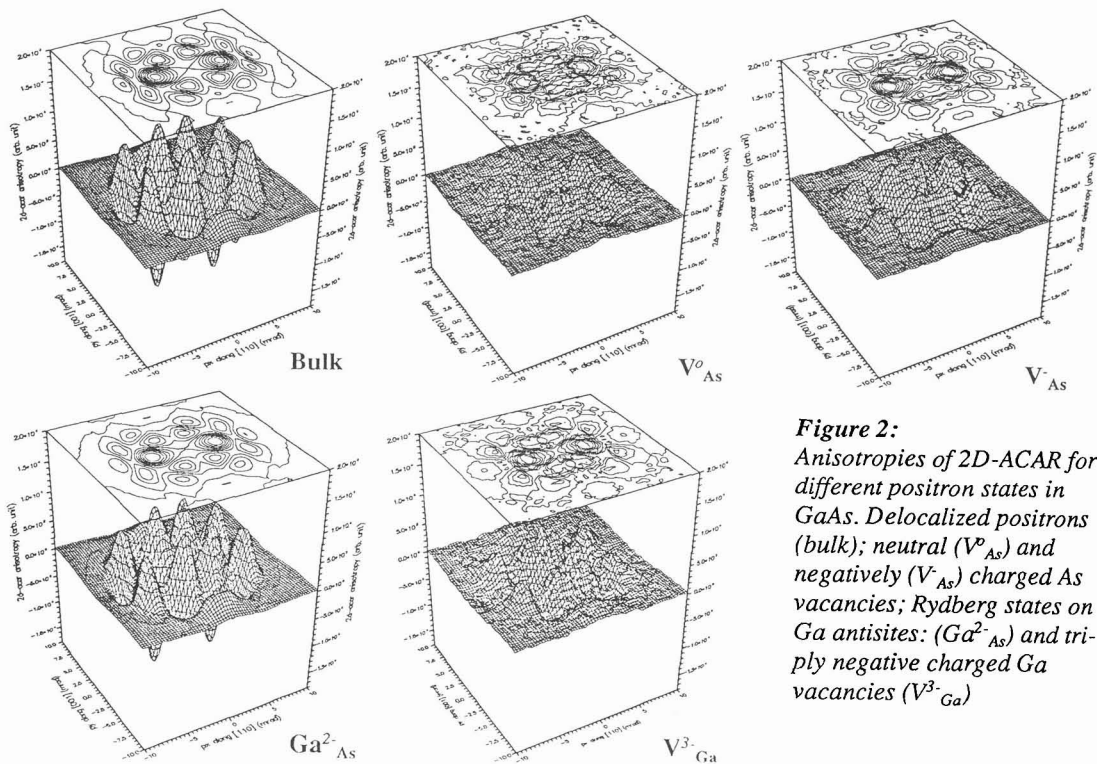


**Figure 2:**  
Anisotropies of 2D-ACAR for different positron states in GaAs. Delocalized positrons (bulk); neutral ( $V_{As}^0$ ) and negatively ( $V_{As}^-$ ) charged As vacancies; Rydberg states on Ga antisites: ( $Ga_{As}^{2-}$ ) and triply negative charged Ga vacancies ( $V_{Ga}^{3-}$ )

smaller for the vacancies.

## 5. DISCUSSION

### 5.1. Annihilation of delocalized positrons

The annihilation of delocalized positrons in GaAs is well understood and from the experimental side good reproducibility is obtained with previous measurements [16]. Various calculations of the theoretical 2D-ACAR distributions have been made. A LCAO approach [17] provides a good description of the observed features. The structures in the central region are the direct consequence of the covalent bonding of the p atomic orbitals. In a compound semiconductor like GaAs, p orbitals from neighboring lattice sites form

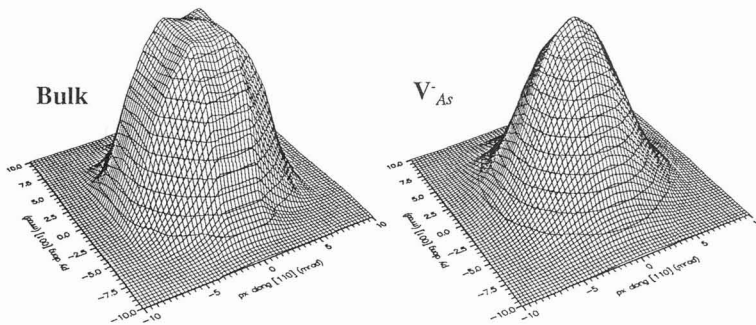


**Figure 3:**  
2D-ACAR distributions calculated using a first-principle molecular dynamics approach (Ref. 6).  
Delocalized positrons (bulk) in GaAs and negatively charged As vacancy ( $V_{As}^-$ )

bonds with a noticeable intensity, unlike in elementary semiconductors where a cancellation occurs because the atoms of the two sites are the same. Other calculations [18] using the pseudopotential method are also in good agreement with the experimental findings and they explain why large anisotropies are obtained for defect-free GaAs, as shown in Figure 2. Recently, a calculation based on a first-principle molecular dynamics calculation has been performed [6]. Although the molecular dynamics method proves, as we shall see below, to be unique for the calculation of the momentum density in defects, it also provides a precise description of the bulk, as shown in Figure 3.

### 5.2. Electronic structure of monovacancies

If the electronic structure of the defect-free GaAs has been well understood for a number of years, the electronic structure of defects, on the other hand, have not been investigated extensively so far. This is mainly due to the difficulty of performing precise first principles electronic structure calculations in a non-periodic structure. 2D-ACAR data require such theoretical investigations if one wants to take full advantage of the information they embody. A very promising approach in this field are Car-Parinello molecular dynamics calculations [7]. Recently, this technique has been used [6] to calculate the 2D-ACAR distribution from positrons trapped in a monovacancy. The case of  $V_{As}^-$  in GaAs has been investigated in a first-principles study of the positron trapping that includes lattice relaxations induced both by the presence of the defect and of the positron. The result of this study is shown in Figure 3, and one immediately notices a clear difference between trapped and free positron states. The shape of the calculated distribution for positron localized in  $V_{As}^-$  is much more isotropic than for delocalized positrons. This is precisely what we find experimentally. This is clear in Figure 1 when one compares with the 2D-ACAR from defect-free GaAs. This is also seen in Figure 2: the anisotropies of  $V_{As}^-$  have smaller amplitudes than the one of defect-free GaAs.

The agreement between measured and calculated 2D-ACAR from vacancies is very encouraging because it opens a new and promising means to study details of the electronic structure of defects in semiconductors.

### 5.3. Relaxation of $V_{As}^-$ and $V_{As}^{\circ}$

The atomic relaxations around the defects can also be investigated with use of 2D-ACAR if one looks at the tails of the distribution (large momentum regions). The reason can be explained by considering the following three points: 1) As core electrons are localized in the real (lattice) space, their momentum density

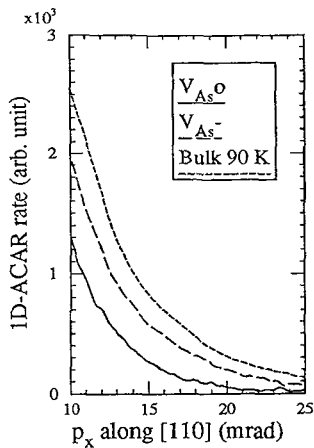


**Figure 4:**  
Tails of 2D-ACAR lines from  
bulk GaAs,  $V_{As}^0$  and  $V_{As}^-$ .

distribution (in the reciprocal lattice space) will be delocalized and be largely predominant in the tails of the 2D-ACAR. 2) The core electrons of the atoms surrounding the vacancy are not affected by the local defect because they are strongly bound to the atom. They can therefore be used as references to study relaxations. 3) The overlap of the wavefunction of the positron localized in a vacancy with the wavefunctions of the surrounding core electrons will depend in first approximation on the distance of the surrounding electrons to the vacancy. As the intensity of the 2D-ACAR is proportional to this overlap, see Eq. (2), we may expect to have an information on the positions of the surrounding atoms. The advantage of 2D-ACAR over the positron lifetime measurements, which also depend on the volume of the vacancy, is that a 2D-ACAR distribution contains directional information. Hence, one should in principle be able to measure the relaxations in various crystallographic directions.

Using these principles, we have investigated the tails of the 2D-ACAR distributions of defect-free GaAs,  $V_{As}^-$  and  $V_{As}^0$ . A typical result is shown in Figure 4 where large differences are obtained, indicating a charge-state-dependent relaxation of the As vacancies in GaAs. We observe that  $V_{As}^-$  yields tail contribu-

tions larger than  $V_{As}^0$ . According to our model, we conclude that  $V_{As}^-$  vacancies suffer a strong inward relaxation. This result is in agreement with first-principles studies of fully relaxed vacancies [19].

#### 5. 4. Positron Rydberg states

Positron lifetime measurements in electron-irradiated GaAs suggest that  $Ga_{As}^{2-}$  gallium antisites act as shallow trapping centers for the positron [14]. In this state the positron is weakly localized in a Rydberg state with a mean diameter that is large compared to the interatomic distance. Therefore, it is expected that the 2D-ACAR will be similar to that of the bulk. This is indeed what is obtained, as shown in Figure 1, where we show the fraction of the 2D-ACAR from a sample of semi-insulating GaAs irradiated with a fluence of  $5 \times 10^{17} \text{ cm}^{-2}$  of 1.5 MeV electrons. Small differences are nevertheless noticed when closely comparing 2D-ACAR anisotropies (Figure 2) from the Rydberg state and from the defect-free (untrapped) positron state. These differences require further investigations for a detailed description of the positron Rydberg state.

## 6. CONCLUSIONS

We have described the 2D-ACAR technique and shown that it is an additional tool to the more traditional lifetime and Doppler broadening measurements in the study of defects in semiconductors by positron annihilation. The main advantages of 2D-ACAR are high resolution and directional sensitivity.

We have outlined some of the capabilities of 2D-ACAR for the study of native vacancies in GaAs. We have shown that the electronic structure of monovacancies can now be investigated both experimentally and theoretically: 2D-ACAR measurements and first-principle molecular dynamics calculations show a qualitative agreement. This opens up a new way for detailed investigations of these electronic structures. We have also obtained information on the charge-related relaxations of the As vacancy in GaAs, which is in agreement with calculations of fully relaxed configurations. Finally, we have shown that 2D-ACAR provides direct evidence for the delocalized nature of the positron Rydberg states (shallow traps) induced by  $Ga_{As}$  antisites.

If direct industrial applications of the 2D-ACAR technique have not yet been implemented, we are convinced that in the future this technique shall find its place beside positron lifetime and Doppler broadening measurements. 2D-ACAR is unique for the studies of defects that depend on crystallographic directions. Moreover, as soon as a controlled implantation of a large flux of positrons will be available [20][21], 2D-ACAR shall provide insights on the electronic properties of epitaxial films, surfaces and interfaces. It is very probable that all these new possibilities shall, in the coming years, trigger lots of progress in the char-



acterization of defects in semiconductors.

### Acknowledgments

We are grateful to M. Peter for his constant support and advice. We thank L. Gilgien, F. Gygi, G. Galli and R. Car for providing us their results prior to publication. We have benefited of enlightening discussions with M. Alatalo, B. Barbiellini, T. Chiba, T. Jarlborg, R.M. Nieminen and S. Tanigawa. This work has been supported by the Swiss National Science Foundation.

### References

- [1] Bourgoin J.C. and von Bardeleben H.J., *J. Appl. Phys.* **64** (1988), R65-R91.
- [2] Hautojärvi P., *Positron Spectroscopy of Solids*, (North-Holland, Amsterdam, 1994), to appear.
- [3] Corbel C., *Positron Spectroscopy of Solids*, (North-Holland, Amsterdam, 1994), to appear.
- [4] Tanigawa S., *Positron Spectroscopy of Solids*, (North-Holland, Amsterdam, 1994), to appear.
- [5] Hautojärvi P., in these proceedings
- [6] Gilgien L. Galli G. Gygi F. and Car R., *Phys. Rev. Lett.* (1994), submitted.
- [7] Car. R. and Parinello M. *Phys. Rev. Lett.* **55** (1985) 2471-2475.
- [8] Ambigapathy R., Manuel A.A., Hautojärvi P., Saarinen K. and Corbel C., *Phys. Rev. B* (1994), submitted.
- [9] For a general reading on the methodology, see Dupasquier A. and Mills A.P., *Positron Spectroscopy of Solids*, (North-Holland, Amsterdam, 1994) and Brandt W. and Dupasquier A., *Positron Solid-State Physics* (North-Holland, Amsterdam, 1983).
- [10] Peter M., *IBM J. of Res. and Dev.*, **33** (1989), 333-341.
- [11] Saarinen K., Hautojärvi P., Lanki P. and Corbel C., *Phys. Rev. B* **44**, 10585 (1991)
- [12] Corbel C., Stucky M., Hautojärvi P., Saarinen K. and Moser P., *Phys. Rev. B* **38**, (1988) 8192
- [13] Puska M.J., Corbel C. and Nieminen R.M., *Phys. Rev. B* **41** (1990) 9980-9993
- [14] Corbel C., Pierre F., Saarinen K. Hautojärvi P. and Moser P., *Phys. Rev. B* **45** (1992) 3386-3399.
- [15] Bisson P.E., Descouts P., Dupanloup A., Manuel A.A., Perréard E., Peter M. and Sachot R., *Helv. Phys. Acta* **55**, (1982) 100.
- [16] Tanigawa S., *Mat. Sci. Forum* **105-110**, (1992) 493-500.
- [17] Chiba T. and Akahane T., *Positron Annihilation*, L. Dorikens-Vanpraet, M. Dorikens and D. Segers, Eds, (World Scientific, Singapore, 1988), pp. 674-676.
- [18] Saito M., Oshiyama A. and Tanigawa S., *Phys. Rev. B* **44**, 10601 (1991)
- [19] Laasonen K., Nieminen R.M. and Puska M.J, *Phys. Rev. B* **45** (1992), 4122
- [20] For a review, see Triftshäuser W. in these proceedings.
- [21] An intense beam is under construction at the Paul-Scherrer Institute, Viligen, Switzerland. See Waerber W.B., Shi M., Taquu D., Zimmermann U., Gerola D., Hegedüs F. and Roellig L.O. *AIP conference proceedings*, (American Institute of Physics, New-York), to appear.